Measurement of Charged and Neutral Current e^-p Deep Inelastic Scattering Cross Sections at High Q^2

The ZEUS Collaboration

M. Derrick[1], D. Krakauer[1], S. Magill[1], D. Mikunas[1], B. Musgrave[1], J. Repond[1], R. Stanek[1], R.L. Talaga[1], H. Zhang[1], R. Ayad[2,a], G. Bari[2], M. Basile[2], L. Bellagamba[2], D. Boscherini[2], A. Bruni[2], G. Bruni[2], P. Bruni[2], G. Cara Romeo[2], G. Castellini[2,b], M. Chiarini[2], L. Cifarelli[3,c], F. Cindolo[2], A. Contin[2], M. Corradi[2], I. Gialas[2], P. Giusti[2], G. Iacobucci[2], G. Laurenti[2], G. Levi[2], A. Margotti[2], T. Massam[2], R. Nania[2], C. Nemoz[2], F. Palmonari[2], A. Polini[2], G. Sartorelli[2], R. Timellini[2], Y. Zamora Garcia[2,a], A. Zichichi[2], A. Bargende[3], J. Crittenden[3], K. Desch[3], B. Diekmann[3,d], T. Doeker[3], M. Eckert[3], L. Feld[3], A. Frey[3], M. Geerts[3], G. Geitz[3,e], M. Grothe[3], T. Haas[3], H. Hartmann[3], D. Haun[3,d], K. Heinloth[3], E. Hilger[3], H.-P. Jakob[3], U.F. Katz[3], S.M. Mari[3], A. Mass[3,f], S. Mengel[3], J. Mollen[3], E. Paul[3], Ch. Rembser[3], R. Schattevoy[3,g], D. Schramm[3], J. Stamm[3], R. Wedemeyer[3], S. Campbell-Robson[4], A. Cassidy[4], N. Dyce[4], B. Foster[4], S. George[4], R. Gilmore[4], G.P. Heath[4], H.F. Heath[4], T.J. Llewellyn[4], C.J.S. Morgado[4], D.J.P. Norman[4], J.A. O'Mara[4], R.J. Tapper[4], S.S. Wilson[4], R. Yoshida[4], R.R. Rau[5], M. Arneodo[6,h], L. Iannotti[6], M. Schioppa[6], G. Susinno[6], A. Bernstein[7], A. Caldwell[7], N. Cartiglia[7], J.A. Parsons[7], S. Ritz[7], F. Sciulli[7], P.B. Straub[7], L. Wai[7], S. Yang[7], Q. Zhu[7], P. Borzemski[8], J. Chwastowski[8], A. Eskreys[8], K. Piotrzkowski[8], M. Zachara[8], L. Zawiejski[8], L. Adamczyk[9], B. Bednarek[9], K. Jeleń[9], D. Kisielewska[9], T. Kowalski[9], E. Rulikowska-Zarębska[9], L. Suszycki[9], J. Zając[9], A. Kotański[10], M. Przybycień[10], L.A.T. Bauerdick[11], U. Behrens[11], H. Beier[11,i], J.K. Bienlein[11], C. Coldewey[11], O. Deppe[11], K. Desler[11], G. Drews[11], M. Flasiński[11,j], D.J. Gilkinson[11], C. Glasman[11], P. Göttlicher[11], J. Grosse-Knetter[11], B. Gutjahr[11], W. Hain[11], D. Hasell[11], H. Hessling[11], H. Hultschig[11], Y. Iga[11], P. Joos[11], M. Kasemann[11], R. Klanner[11], W. Koch[11], L. Köpke[11,k], U. Kötz[11], H. Kowalski[11], J. Labs[11], A. Ladage[11], B. Löhr[11], M. Löwe[11], D. Lüke[11], O. Mańczak[11], J.S.T. Ng[11], S. Nickel[11], D. Notz[11], K. Ohrenberg[11], M. Roco[11], M. Rohde[11], J. Roldán[11], U. Schneekloth[11], W. Schulz[11], F. Selonke[11], E. Stiliaris[11,l], B. Surrow[11], T. Voss[11], D. Westphal[11], G. Wolf[11], C. Youngman[11], J.F. Zhou[11], H.J. Grabosch[12], A. Kharchilava[12], A. Leich[12], M. Mattingly[12], A. Meyer[12], S. Schlenstedt[12], N. Wulff[12], G. Barbagli[13], P. Pelfer[13], G. Anzivino[14], G. Maccarrone[14], S. De Pasquale[14], L. Votano[14], A. Bamberger[15], S. Eisenhardt[15], A. Freidhof[15], S. Söldner-Rembold[15,m], J. Schroeder[15,n], T. Trefzger[15], N.H. Brook[16], P.J. Bussey[16], A.T. Doyle[16,o], J.I. Fleck[16], D.H. Saxon[16], M.L. Utley[16], A.S. Wilson[16], A. Dannemann[17], U. Holm[17], D. Horstmann[17], T. Neumann[17], R. Sinkus[17], K. Wick[17], E. Badura[18,p], B.D. Burow[18,q], L. Hagge[18], E. Lohrmann[18], J. Mainusch[18], J. Milewski[18], M. Nakahata[18,r], N. Pavel[18], G. Poelz[18], W. Schott[18], F. Zetsche[18], T.C. Bacon[19], I. Butterworth[19], E. Gallo[19], V.L. Harris[19], B.Y.H. Hung[19], K.R. Long[19], D.B. Miller[19], P.P.O. Morawitz[19], A. Prinias[19], J.K. Sedgbeer[19], A.F. Whitfield[19], U. Mallik[20], E. McCliment[20], M.Z. Wang[20], S.M. Wang[20], J.T. Wu[20], Y. Zhang[20], P. Cloth[21], D. Filges[21], S.H. An[22], S.M. Hong[22], S.W. Nam[22], S.K. Park[22], M.H. Suh[22], S.H. Yon[22], R. Imlay[23], S. Kartik[23], H.-J. Kim[23], R.R. McNeil[23], W. Metcalf[23], V.K. Nadendla[23], F. Barreiro[24,s], G. Cases[24], R. Graciani[24], J.M. Hernández[24], L. Hervás[24,s], L. Labarga[24,s], J. del Peso[24], J. Puga[24], J. Terron[24], J.F. de Trocóniz[24], G.R. Smith[25], F. Corriveau[26], D.S. Hanna[26], J. Hartmann[26], L.W. Hung[26], J.N. Lim[26], C.G. Matthews[26], P.M. Patel[26], L.E. Sinclair[26], D.G. Stairs[26], M. St.Laurent[26], R. Ullmann[26], G. Zacek[26], V. Bashkirov[27], B.A. Dolgoshein[27], A. Stifutkin[27], G.L. Bashindzhagyan[28], P.F. Ermolov[28], L.K. Gladilin[28], Y.A. Golubkov[28], V.D. Kobrin[28], V.A. Kuzmin[28], A.S. Proskuryakov[28], A.A. Savin[28], L.M. Shcheglova[28], A.N. Solomin[28], N.P. Zotov[28], M. Botje[29], F. Chlebana[29], A. Dake[29], J. Engelen[29], M. de Kamps[29], P. Kooijman[29], A. Kruse[29], H. Tiecke[29], W. Verkerke[29], M. Vreeswijk[29], L. Wiggers[29], E. de Wolf[29], R. van Woudenberg[29], D. Acosta[30], B. Bylsma[30], L.S. Durkin[30], K. Honscheid[30], C. Li[30], T.Y. Ling[30], K.W. McLean[30,t], W.N. Murray[30], I.H. Park[30], T.A. Romanowski[30,u], R. Seidlein[30,v], D.S. Bailey[31], G.A. Blair[31,w], A. Byrne[31], R.J. Cashmore[31], A.M. Cooper-Sarkar[31], D. Daniels[31,x], R.C.E. Devenish[31], N. Harnew[31], M. Lancaster[31], P.E. Luffman[31,y], L. Lindemann[31], J.D. McFall[31], C. Nath[31], V.A. Noyes[31], A. Quadt[31], H. Uijterwaal[31], R. Walczak[31], F.F. Wilson[31], T. Yip[31], G. Abbiendi[32], A. Bertolin[32], R. Brugnera[32], R. Carlin[32], F. Dal Corso[32], M. De Giorgi[32], U. Dosselli[32], S. Limentani[32], M. Morandin[32], M. Posocco[32], L. Stanco[32], R. Stroili[32], C. Voci[32], J. Bulmahn[33], J.M. Butterworth[33], R.G. Feild[33], B.Y. Oh[33], J.J. Whitmore[33,z], G. D'Agostini[34], G. Marini[34], A. Nigro[34], E. Tassi[34], J.C. Hart[35], N.A. McCubbin[35], K. Prytz[35], T.P. Shah[35], T.L. Short[35], E. Barberis[36], T. Dubbs[36], C. Heusch[36], M. Van Hook[36], B. Hubbard[36], W. Lockman[36], J.T. Rahn[36], H.F.-W. Sadrozinski[36], A. Seiden[36], J. Biltzinger[37], R.J. Seifert[37], A.H. Walenta[37], G. Zech[37], H. Abramowicz[38], G. Briskin[38], S. Dagan[38,*], A. Levy[38,†], T. Hasegawa[39], M. Hazumi[39], T. Ishii[39], M. Kuze[39], S. Mine[39], Y. Nagasawa[39], M. Nakao[39], I. Suzuki[39], K. Tokushuku[39], S. Yamada[39], Y. Yamazaki[39], M. Chiba[40], R. Hamatsu[40], T. Hirose[40], K. Homma[40], S. Kitamura[40], Y. Nakamitsu[40], K. Yamauchi[40], R. Cirio[41], M. Costa[41], M.I. Ferrero[41], L. Lamberti[41], S. Maselli[41], C. Peroni[41], R. Sacchi[41], A. Solano[41], A. Staiano[41], M. Dardo[42], D.C. Bailey[43], D. Bandyopadhyay[43], F. Benard[43], M. Brkic[43], M.B. Crombie[43], D.M. Gingrich[43,‡], G.F. Hartner[43], K.K. Joo[43], G.M. Levman[43], J.F. Martin[43], R.S. Orr[43], C.R. Sampson[43], R.J. Teuscher[43], C.D. Catterall[44], T.W. Jones[44], P.B. Kaziewicz[44], J.B. Lane[44], R.L. Saunders[44], J. Shulman[44], K. Blankenship[45], J. Kochocki[45], B. Lu[45], L.W. Mo[45], W. Bogusz[46], K. Charchuła[46], J. Ciborowski[46], J. Gajewski[46], G. Grzelak[46], M. Kasprzak[46], M. Krzyżanowski[46], K. Muchorowski[46], R.J. Nowak[46], J.M. Pawlak[46], T. Tymieniecka[46], A.K. Wróblewski[46], J.A. Zakrzewski[46], A.F. Żarnecki[46], M. Adamus[47], Y. Eisenberg[48,*], U. Karshon[48,*], D. Revel[48,*], D. Zer-Zion[48], I. Ali[49], W.F. Badgett[49], B. Behrens[49], S. Dasu[49], C. Fordham[49], C. Foudas[49], A. Goussiou[49], R.J. Loveless[49], D.D. Reeder[49], S. Silverstein[49], W.H. Smith[49], A. Vaiciulis[49], M. Wodarczyk[49], T. Tsurugai[50], S. Bhadra[51], M.L. Cardy[51], C.-P. Fagerstroem[51], W.R. Frisken[51], K.M. Furutani[51], M. Khakzad[51], W.B. Schmidke[51]

[1] *Argonne National Laboratory, Argonne, IL, USA*
[2] *University and INFN Bologna, Bologna, Italy*
[3] *Physikalisches Institut der Universität Bonn, Bonn, Federal Republic of Germany*
[4] *H.H. Wills Physics Laboratory, University of Bristol, Bristol, U.K.*
[5] *Brookhaven National Laboratory, Upton, L.I., USA*

[6] Calabria University, Physics Dept.and INFN, Cosenza, Italy
[7] Columbia University, Nevis Labs., Irvington on Hudson, N.Y., USA
[8] Inst. of Nuclear Physics, Cracow, Poland
[9] Faculty of Physics and Nuclear Techniques, Academy of Mining and Metallurgy, Cracow, Poland
[10] Jagellonian Univ., Dept. of Physics, Cracow, Poland
[11] Deutsches Elektronen-Synchrotron DESY, Hamburg, Federal Republic of Germany
[12] DESY-Zeuthen, Inst. für Hochenergiephysik, Zeuthen, Federal Republic of Germany
[13] University and INFN, Florence, Italy
[14] INFN, Laboratori Nazionali di Frascati, Frascati, Italy
[15] Fakultät für Physik der Universität Freiburg i.Br., Freiburg i.Br., Federal Republic of Germany
[16] Dept. of Physics and Astronomy, University of Glasgow, Glasgow, U.K.
[17] Hamburg University, I. Institute of Exp. Physics, Hamburg, Federal Republic of Germany
[18] Hamburg University, II. Institute of Exp. Physics, Hamburg, Federal Republic of Germany
[19] Imperial College London, High Energy Nuclear Physics Group, London, U.K.
[20] University of Iowa, Physics and Astronomy Dept., Iowa City, USA
[21] Forschungszentrum Jülich, Institut für Kernphysik, Jülich, Federal Republic of Germany
[22] Korea University, Seoul, Korea
[23] Louisiana State University, Dept. of Physics and Astronomy, Baton Rouge, LA, USA
[24] Univer. Autónoma Madrid, Depto de Física Teóríca, Madrid, Spain
[25] University of Manitoba, Dept. of Physics, Winnipeg, Manitoba, Canada
[26] McGill University, Dept. of Physics, Montréal, Québec, Canada
[27] Moscow Engineering Physics Institute, Mosocw, Russia
[28] Moscow State University, Institute of Nuclear Physics, Moscow, Russia
[29] NIKHEF and University of Amsterdam, Netherlands
[30] Ohio State University, Physics Department, Columbus, Ohio, USA
[31] Department of Physics, University of Oxford, Oxford, U.K.
[32] Dipartimento di Fisica dell' Universita and INFN, Padova, Italy
[33] Pennsylvania State University, Dept. of Physics, University Park, PA, USA
[34] Dipartimento di Fisica, Univ. 'La Sapienza' and INFN, Rome, Italy
[35] Rutherford Appleton Laboratory, Chilton, Didcot, Oxon, U.K.
[36] University of California, Santa Cruz, CA, USA
[37] Fachbereich Physik der Universität-Gesamthochschule Siegen, Federal Republic of Germany
[38] School of Physics,Tel-Aviv University, Tel Aviv, Israel
[39] Institute for Nuclear Study, University of Tokyo, Tokyo, Japan
[40] Tokyo Metropolitan University, Dept. of Physics, Tokyo, Japan
[41] Universita di Torino, Dipartimento di Fisica Sperimentale and INFN, Torino, Italy
[42] II Faculty of Sciences, Torino University and INFN - Alessandria, Italy
[43] University of Toronto, Dept. of Physics, Toronto, Ont., Canada
[44] University College London, Physics and Astronomy Dept., London, U.K.
[45] Virginia Polytechnic Inst. and State University, Physics Dept., Blacksburg, VA, USA

[46] *Warsaw University, Institute of Experimental Physics, Warsaw, Poland*
[47] *Institute for Nuclear Studies, Warsaw, Poland*
[48] *Weizmann Institute, Nuclear Physics Dept., Rehovot, Israel*
[49] *University of Wisconsin, Dept. of Physics, Madison, WI, USA*
[50] *Meiji Gakuin University, Faculty of General Education, Yokohama, Japan*
[51] *York University, Dept. of Physics, North York, Ont., Canada*

(MARCH 30, 1995)

Abstract

Deep inelastic e^-p scattering has been studied in both the charged-current (CC) and neutral-current (NC) reactions at momentum transfers squared, Q^2, between 400 GeV^2 and the kinematic limit of 87500 GeV^2 using the ZEUS detector at the HERA ep collider. The CC and NC total cross sections, the NC to CC cross section ratio, and the differential cross sections, $d\sigma/dQ^2$, are presented. For $Q^2 \simeq M_W^2$, where M_W is the mass of the W boson, the CC and NC cross sections have comparable magnitudes, demonstrating the equal strengths of the weak and electromagnetic interactions at high Q^2. The Q^2-dependence of the CC cross section determines the mass term in the CC propagator to be $M_W = 76 \pm 16 \pm 13$ GeV.

Typeset using REVTEX

Lepton-nucleon scattering is an important technique for studying the constituents of the nucleon and their interactions. In the Standard Model [1], electron-proton (ep) scattering occurs via the exchange of gauge bosons (γ, Z^0, $W^\pm$). At long wavelengths (small momentum transfers), interactions of the massless photon dominate over the exchange of the heavy gauge bosons. However, at the ep storage ring HERA, for the first time, scattering can be observed at sufficiently short wavelengths (large momentum transfers) that the 'weak' and 'electromagnetic' scattering cross sections have comparable magnitudes.

Neglecting longitudinal structure functions and radiative corrections, the differential cross section for deep inelastic scattering (DIS) with unpolarized e^-p beams can be expressed as [2]:

$$\frac{d^2\sigma}{dx dQ^2} = \frac{2\pi\alpha^2}{xQ^4}\left[\{1+(1-y)^2\}\mathcal{F}_2 + \{1-(1-y)^2\}x\mathcal{F}_3\right]$$

where the $\mathcal{F}_i(x,Q^2)$ functions describe the proton structure and couplings. In this equation, Q^2 is the negative square of the four-momentum transfer, y is the fractional energy transfer from the lepton in the proton rest frame, α is the electromagnetic fine-structure constant and x in the quark-parton model is the momentum fraction of the proton carried by the quark struck by the exchanged boson. These variables are related by $Q^2 = sxy$, where $\sqrt{s}$ is the center-of-mass energy. The $\mathcal{F}_i$ can be expressed as sums over quark flavors, f, of the quark densities inside the proton, $q_f(x,Q^2)$, weighted according to the gauge structure of the scattering amplitudes. For the neutral-current (NC) reaction, $e^-p \to e^-X$, mediated by γ and Z^0 exchange, they can be written as:

$$\mathcal{F}_2^{NC} = \sum_f q_f^+\left[e_f^2 + 2v_e v_f e_f \mathcal{P}_Z + (v_e^2+a_e^2)(v_f^2+a_f^2)\mathcal{P}_Z^2\right]$$

$$x\mathcal{F}_3^{NC} = \sum_f q_f^-\left[-2a_e a_f e_f \mathcal{P}_Z + (4v_e a_e v_f a_f)\,\mathcal{P}_Z^2\right]$$

where $q_f^\pm = \{xq_f(x,Q^2) \pm x\bar{q}_f(x,Q^2)\}$, a_e and v_e are the axial- and vector-couplings of the e^- to the Z^0, and a_f and v_f are the analogous couplings for a quark of flavor f which has electric charge e_f [1]. $\mathcal{P}_Z$ is the ratio of Z^0-to-photon propagators, given by $\mathcal{P}_Z = Q^2/(Q^2 + M_Z^2)$, where M_Z is the mass of the Z boson.

For charged-current (CC) scattering, $e^- p \to \nu_e X$, in which $W^\pm$ bosons are exchanged, the functions are:

$$\mathcal{F}_2^{CC} = \frac{x\mathcal{P}_W^2}{8\sin^4\theta_W} \sum_{k,m} \left[|V_{km}|^2 u_k + |V_{mk}|^2 \bar{d}_m \right]$$

$$x\mathcal{F}_3^{CC} = \frac{x\mathcal{P}_W^2}{8\sin^4\theta_W} \sum_{k,m} \left[|V_{km}|^2 u_k - |V_{mk}|^2 \bar{d}_m \right]$$

where k and m are the generation indices of up-type quarks, $u_k(x, Q^2)$, and down-type antiquarks, $\bar{d}_m(x, Q^2)$, V is the Cabibbo-Kobayashi-Maskawa quark mixing matrix, θ_W is the weak mixing angle, and $\mathcal{P}_W = Q^2/(Q^2+M_W^2)$. At lowest order, $G_F M_W^2 = \pi\alpha/\sqrt{2}\sin^2\theta_W$, where G_F is the Fermi constant.

In 1993, HERA collided 26.7 GeV e^- with 820 GeV p, giving $\sqrt{s} = 296$ GeV. Due to this high center-of-mass energy, DIS can be investigated at much higher Q^2 at HERA than in existing fixed target experiments. The predicted DIS cross sections at fixed x over a large Q^2 range depend both on the electroweak theory for the propagators and couplings and on Quantum Chromodynamics (QCD) for the parton density evolution. The structure functions, $\mathcal{F}_2$, have been measured [3] in ep and μp scattering up to $Q^2 \sim 5(150)$ GeV^2 for $x = 0.03(0.3)$. The parton density distributions [4,5] inferred from those measurements were extrapolated to our Q^2 region using the next-to-leading-order QCD evolution equations [6]. At x of 0.03 (0.3), the up-quark density is predicted to change by 21% (−39%) as Q^2 increases from 5 GeV^2 to 16000 GeV^2. In contrast, the NC propagator varies by 7 orders of magnitude over the same Q^2 interval.

This paper reports measurements of integrated and differential cross sections, $d\sigma/dQ^2$, for NC and CC DIS with $Q^2 > 400$ GeV^2 using a luminosity of 0.540 ± 0.016 pb^{-1}. ZEUS [7] and H1 [8] have previously reported on NC DIS cross section measurements at lower Q^2. The H1 experiment has also measured the CC total cross section [9] and demonstrated that at large Q^2 the mass in the CC propagator is finite.

ZEUS [10] is a multipurpose, magnetic detector, designed especially to measure DIS. Charged particles are tracked by drift chambers operating in an axial magnetic field of 1.43 T. The superconducting solenoid is surrounded by a compensating uranium-scintillator calorimeter (CAL) with an electromagnetic (hadronic) energy resolution of $18\%/\sqrt{E(\mathrm{GeV})}$ $(35\%/\sqrt{E(\mathrm{GeV})})$ and a subnanosecond time resolution. The CAL covers the angular range between 2.2° and 176.5°. ZEUS used a right-handed coordinate system, centered at the nominal interaction point ($z = 0$), defined with positive z along the direction of the proton beam and positive y upwards. The CAL is segmented in depth into electromagnetic and hadronic sections, with a total thickness of 4 to 7 interaction lengths. Surrounding the CAL is an iron magnetic return yoke instrumented for muon detection. For this analysis, the muon detectors were used to identify cosmic-ray induced triggers. The luminosity is measured by the rate of high-energy photons from the reaction $ep \rightarrow ep\gamma$ detected in a lead-scintillator calorimeter located $z = -107$ m from the interaction region.

Data were collected with a three-level trigger. The first-level trigger was based on electromagnetic energy, transverse energy and total energy deposits in the CAL [7]. The thresholds, between 2 and 15 GeV, were well below the offline selection cuts. The second-level trigger rejected p-gas events (proton interactions with residual gas in the beam pipe upstream of the detector) recognized by CAL energy deposited at times early relative to that of the ep crossing. The third-level trigger selected events as NC DIS candidates if $E - P_z$ exceeded 25 GeV, where E and P_z are the summed energy and z-component of the momentum measured in the calorimeter. If no energy escapes through the rear beam hole, $E - P_z \approx 2E_e$ where E_e is the electron beam energy. Events were selected as CC DIS candidates if $\not{P}_t$, the absolute value of the missing transverse momentum measured by the calorimeter, exceeded 9 GeV, and there was either more than 10 GeV deposited in the forward part of CAL or at least one track reconstructed in the drift chambers.

As the ZEUS detector is nearly hermetic, it is possible to reconstruct the kinematic variables x and Q^2 for NC DIS using different combinations of the angles and energies of the scattered lepton and hadronic system [7]. Three methods were relevant to this analysis. The electron (e) method uses E'_e and θ_e, the energy and polar angle of the scattered electron. The hadronic, or Jacquet-Blondel (JB) [11], method reconstructs y and Q^2 as $y_{JB} = (E_h - P_{z,h})/(2E_e)$ and $Q^2_{JB} = P^2_{t,h}/(1 - y_{JB})$, where E_h, $P_{z,h}$ and $P_{t,h}$ are the energy, the $z-$component of momentum, and the transverse momentum, of the hadronic system. The double angle (DA) method uses θ_e and γ_h, the polar angle of the struck quark which is given by $\cos\gamma_h = (P^2_{t,h} - (2E_e y_{JB})^2)/(P^2_{t,h} + (2E_e y_{JB})^2)$. The DA method, which measures Q^2 with small bias and good resolution, was used to reconstruct NC events [7]. For CC DIS, the hadronic (JB) method was used.

The acceptances and measurement resolutions for signal and background events were determined using Monte Carlo methods. Simulated CC and NC DIS events, generated using LEPTO [12] interfaced to HERACLES [13] by DJANGO [14], were passed through a GEANT [15] based detector simulation, and subsequently analyzed with the same reconstruction and offline selection procedures as the data. The calculated efficiencies and acceptances were found to have negligible dependences on either the model of the hadronic final state [12,16] or the proton parton density parametrizations [4] used in the simulation.

The offline NC DIS event selection required an electron candidate with $E'_e > 10$ GeV in the calorimeter and $E - P_z > 35$ GeV. To reject backgrounds from photoproduction events with a fake electron (mostly π^0's at small polar angles) the electron candidate was required to have a matching track and to satisfy $y_e < 0.95$. Cosmic-ray triggers were rejected by requiring $\not{P}_t/\sqrt{E_t} < 2$ GeV$^{\frac{1}{2}}$. A final cut required Q^2, as reconstructed by the DA and e methods, to be consistent: $0.7 < Q^2_e/Q^2_{DA} < 1.2$. After these selections, 436 events with $Q^2_{DA} > 400$ GeV^2 remained. The photoproduction background is less than 2%. Over the full y range of $0 < y < 1$, more than 85% of all Monte Carlo NC DIS events with $Q^2 > 400$ GeV^2 pass all of the above cuts. The spectra of x and Q^2 for the data and the Monte Carlo simulation are shown in Figures 1a,b. The agreement is satisfactory in both shape and absolute magnitude.

The NC DIS cross sections in five bins of Q^2 between 400 GeV^2 and the kinematic limit at 87500 GeV^2 are given in Table I. The cross section was calculated for each bin as

$\sigma_{NC} = (N_{NC} \cdot \delta r_{NC})/(\mathcal{L} \cdot \mathcal{A}_{NC})$ where N_{NC} is the number of NC DIS events reconstructed in the bin, δr_{NC} is the radiative correction, and $\mathcal{L}$ is the luminosity. The acceptance for the bin, $\mathcal{A}_{NC}$, was calculated from the NC DIS Monte Carlo event sample, as the ratio of the number of events which pass all cuts and have the reconstructed Q^2_{DA} in the bin to the number of events with the true Q^2 in the bin. $\mathcal{A}_{NC}$ varies between 0.79 and 0.85. HERACLES [13] was used to calculate the radiative correction factor, δr_{NC}, which was in the range 0.88 to 0.95 and has been applied to the data in order to obtain Born cross sections.

The systematic errors on $\mathcal{A}_{NC}$ include: a 4% error assigned to the uncertainty of the calorimeter energy response; a 3% uncertainty assigned to the efficiency of the calorimeter-track matching for the electron; a 4% error for the efficiency of the electron finding algorithm; and a 5% error in the lowest Q^2 bin for the uncertainty in the efficiency of the Q^2_e/Q^2_{DA} cut.

The CC DIS events are characterized by a large $\not{p}_t$ due to the final-state neutrino. The 36000 triggers for this mode were produced predominantly by upstream p-gas interactions or cosmic rays. The offline CC DIS selection required $\not{p}_t > 12$ GeV and a vertex, formed from two or more tracks, within 45 cm of the nominal interaction point. Events with more than 40 tracks not associated with the vertex were rejected. To reduce the remaining p-gas background, for which the reconstructed transverse energy was concentrated at small polar angles, events with $\not{p}_t^{outer} < 0.7\not{p}_t$ were rejected, where $\not{p}_t^{outer}$ is the missing transverse momentum in the calorimeter excluding the 1.0×1.0 m^2 region around the forward beam pipe. The 117 candidates remaining were mostly cosmic-ray events, including cosmic-ray muons coincident with a p-gas interaction. Single muons were rejected on the basis of their characteristic spatial distribution of energy deposition in the calorimeter. Additionally, the times of all energy deposits measured in the calorimeter were required to be consistent with a single ep interaction. Events with track segments in three or more muon chambers were also rejected.

The events passing all selection criteria were scanned and one cosmic-ray event was removed, leaving 23 events with $Q^2 > 400$ GeV^2 in the final CC DIS sample. From Monte Carlo simulations, we expect fewer than one background event from photoproduction.

The hadronic energies in CC events were corrected for energy loss in material between the vertex and the calorimeter with a multiplicative factor which depended on the uncorrected $P_{t,h}$ and $E_h - P_{z,h}$. The correction was determined using NC DIS events, for which the hadronic four-momentum can be reconstructed using the DA method. The correction factor varies between 1.03 (at small $E_h - P_{z,h}$) and 1.22 (at small $P_{t,h}$). Figures 1c, d show the reconstructed x and Q^2 distributions for CC DIS sample with $Q^2 > 400$ GeV^2 compared to the Monte Carlo simulation. Within the limited statistics of the data, the agreement is satisfactory.

The CC DIS cross sections, $\sigma_{CC} = (N_{CC} \cdot \delta r_{CC})/(\mathcal{L} \cdot \mathcal{A}_{CC})$, are shown in Table I. The acceptance, $\mathcal{A}_{CC}$, is in the range 0.67 to 0.80, except for the bin at largest Q^2 where it is 1.10 due to migration from lower Q^2. Seventy-five percent of Monte Carlo CC DIS events generated with $Q^2 > 400$ GeV^2 pass all of the selection cuts. The systematic errors on $\mathcal{A}_{CC}$ include: a 5% estimated uncertainty from the dependence on the $\not{P}_t$ and the $\not{P}_t^{outer}/\not{P}_t$ thresholds; a 5% assigned error on the efficiency to reconstruct a vertex with two tracks; an 8% error in the lowest Q^2 bin due to the calorimeter energy scale; and a 9% (20%) error on the lower four bins (highest Q^2 bin) due to uncertainties in the hadronic energy correction. A radiative correction factor, δr_{CC}, in the range 1.02 to 1.03 has been applied to the visible cross section in each bin in order to report a Born cross section.

The differential Born cross sections $d\sigma/dQ^2$ for both NC and CC scattering are shown in Figure 2. The measured cross sections agree with the Standard Model predictions. The ratios of the NC to CC total cross sections for $Q^2 > Q^2_{min}$ are listed in Table I. From the lowest bin in Q^2 to the highest (for which $Q^2 \simeq M_W^2$), the ratio of $d\sigma_{NC}/dQ^2$ to $d\sigma_{CC}/dQ^2$ decreases by two orders of magnitude to around unity, thus demonstrating the equal strengths of the weak and electromagnetic forces at high Q^2.

The rapid fall of the NC cross section with increasing Q^2 is mainly due to the massless photon propagator, as can be seen from the contribution to the NC cross section from photon exchange only, σ^{γ}_{NC} in Table I. The Q^2-dependence of the CC cross section is sensitive to the mass, M_W, in the CC propagator. The CC cross sections expected in the limit of infinite propagator mass, $\sigma_{CC}^{M_W\to\infty}$, are inconsistent with the data, as shown in Table I. Fitting $d\sigma_{CC}/dQ^2$ with M_W as the free parameter, and G_F fixed, we find $M_W = 76\pm16(stat)\pm13(syst)$ GeV, which agrees with the $W^\pm$ mass, $M_W = 80.22\pm0.26$ GeV [17], measured at hadron colliders.

The ZEUS experiment has been made possible by the ingenuity and dedicated effort of many people from inside DESY and from the outside institutes who are not listed here as authors. Their contributions are deeply appreciated, as are the inventiveness and continued diligent efforts of the HERA machine group and the DESY network computing services. We thank the DESY directorate for strong support and encouragement.

REFERENCES

[a] supported by Worldlab, Lausanne, Switzerland

[b] also at IROE Florence, Italy

[c] now at Univ. of Salerno and INFN Napoli, Italy

[d] now a self-employed consultant

[e] on leave of absence

[f] now at Institut für Hochenergiephysik, Univ. Heidelberg

[g] now at MPI Berlin

[h] now also at University of Torino

[i] presently at Columbia Univ., supported by DAAD/HSPII-AUFE

[j] now at Inst. of Computer Science, Jagellonian Univ., Cracow

[k] now at Univ. of Mainz

[l] supported by the European Community

[m] now at Faculty of Physics at Univ. of Freiburg

[n] now at SAS-Institut GmbH, Heidelberg

[o] also supported by DESY

[p] now at GSI Darmstadt

[q] also supported by NSERC

[r] now at Institute for Cosmic Ray Research, University of Tokyo

[s] on leave of absence at DESY, supported by DGICYT

[t] now at Carleton University, Ottawa, Canada

[u] now at Department of Energy, Washington

[v] now at HEP Div., Argonne National Lab., Argonne, IL, USA

[w] now at RHBNC, Univ. of London, England

[x] Fulbright Scholar 1993-1994

[y] now at Cambridge Consultants, Cambridge, U.K.

[z] on leave and partially supported by DESY 1993-95

[*] supported by a MINERVA Fellowship

[†] partially supported by DESY

‡ now at Centre for Subatomic Research, Univ.of Alberta, Canada and TRIUMF, Vancouver, Canada

[1] A concise summary of the Standard Model of electroweak interactions can be found in L. Montanet et al., Particle Data Group, Phys. Rev. **D50**, 1304 (1994).

[2] G. Ingelman and R. Rückl, Phys. Lett. **B201**, 369 (1988).

[3] J. Feltesse, Rapporteur talk at 24th International Conference on High Energy Physics, Glasgow, July 20-27, 1994, DAPNIA/SPP 94-35.

[4] A. D. Martin, W. J. Stirling, and R. G. Roberts, Phys. Lett. **B306**, 145 (1993).

[5] CTEQ Collaboration, H.L. Lai et al., Michigan State University preprint, MSU-HEP-41024, October 1994. M. Glück, E. Reya and A. Vogt, Phys. Lett. **B306**, 391 (1993).

[6] V. Gribov and L. Lipatov, Sov. J. Nucl. Phys. **15**, 438 (1972); G. Altarelli and G. Parisi, Nucl. Phys. **B126**, 298 (1977).

[7] ZEUS Collaboration, M. Derrick et al., Z. Phys. **C65**, 379 (1995).

[8] H1 Collaboration, I. Abt et al., DESY 95-006 (submitted to Nucl. Phys. B).

[9] H1 Collaboration, I. Abt et al., Phys. Lett. **B324**, 241 (1994).

[10] The ZEUS Detector, Status Report 1993, DESY 1993.

[11] F. Jacquet and A. Blondel, in Proceedings of the study for an ep facility in Europe 79/48 (1979) 391, ed. U. Amaldi.

[12] LEPTO 6.1 with the matrix element plus parton shower option: G. Ingelman, Proc. of the Workshop on Physics at HERA, ed. W. Buchmüller and G. Ingelman. (DESY, Hamburg 1992) vol. 3, 1366.

[13] HERACLES 4.1: A. Kwiatkowski, H. Spiesberger, H.-J. Möhring, in Physics at HERA, *ibid.*, vol. 3, 1294.

[14] DJANGO 1.0: G. Schuler and H. Spiesberger, in Physics at HERA, *ibid.*, vol. 3, 1419.

[15] GEANT 3.13: R. Brun et al., CERN DD/EE-84-1 (1987).

[16] ARIADNE with the Color Dipole + Boson Gluon Fusion model: L. Lönnblad, Comp. Phys. Comm. **71**, 15 (1992).

[17] The Particle Data Group, L. Montanet et al., Phys. Rev. **D50**, 1351 (1994).

Q^2_{min}, Q^2_{max} (GeV^2)	400, 1000	1000, 2500	2500, 6250	6250, 15625	15625, 87500
N_{NC}	328	86	18	3	1
$\sigma^{meas}_{NC}(pb)$	$629 \pm 38 \pm 69$	$163 \pm 18 \pm 15$	$36 \pm 9 \pm 4$	$5.8\ ^{+3.6}_{-3.2} \pm 0.6$	$2.0\ ^{+2.9}_{-1.6} \pm 0.3$
δr_{NC}	0.89	0.88	0.89	0.91	0.95
$\sigma^{SM}_{NC}(pb)$	644	167	41	8.8	1.1
$\sigma^{\gamma}_{NC}(pb)$	636	159	35	5.9	0.6
N_{CC}	2	7	5	7	2
$\sigma^{meas}_{CC}(pb)$	$5.8\ ^{+4.6}_{-3.8} \pm 0.9$	$16.8\ ^{+6.7}_{-6.1} \pm 2.3$	$12.3\ ^{+5.8}_{-5.3} \pm 1.7$	$16.8\ ^{+6.7}_{-6.1} \pm 2.2$	$3.4\ ^{+2.7}_{-2.1} \pm 0.8$
δr_{CC}	1.02	1.03	1.03	1.03	1.02
$\sigma^{SM}_{CC}(pb)$	13.3	17.1	15.9	8.0	1.6
$\sigma^{M_W \to \infty}_{CC}(pb)$	17.5	28.3	41.8	46.0	21.2
$\sigma_{NC}(Q^2 > Q^2_{min})$	837 ± 100	209 ± 27	46 ± 12	8.0 ± 4.1	2.0 ± 1.7
$\sigma_{CC}(Q^2 > Q^2_{min})$	57 ± 20	50 ± 13	34 ± 10	21 ± 3.1	3.4 ± 2.7
$R\left(\frac{\sigma_{NC}}{\sigma_{CC}}\right)_{Q^2 > Q^2_{min}}$	$14.7^{+3.4}_{-3.2}$	$4.2^{+1.3}_{-0.9}$	$1.4^{+0.6}_{-0.4}$	$0.4^{+0.3}_{-0.1}$	$0.7^{+1.0}_{-0.5}$

TABLE I. Events observed and integrated Born cross sections for NC and CC DIS. Errors shown are statistical, followed by systematic (which includes the 3.5% luminosity uncertainty). The Born cross sections were obtained from the visible cross sections by multiplying by the radiative correction factor, $\delta r_{NC,CC}$. The Standard Model (SM) cross sections are calculated with LEPTO [12] using the MRSD$'_-$ parton distributions [4]. The predictions for a photon-only NC σ^{γ}_{NC}, and for an infinite mass in the CC propagator $\sigma^{M_W \to \infty}_{CC}$, are also shown. The NC to CC cross sections and their ratios, R, are also given for $Q^2 > Q^2_{min}$.

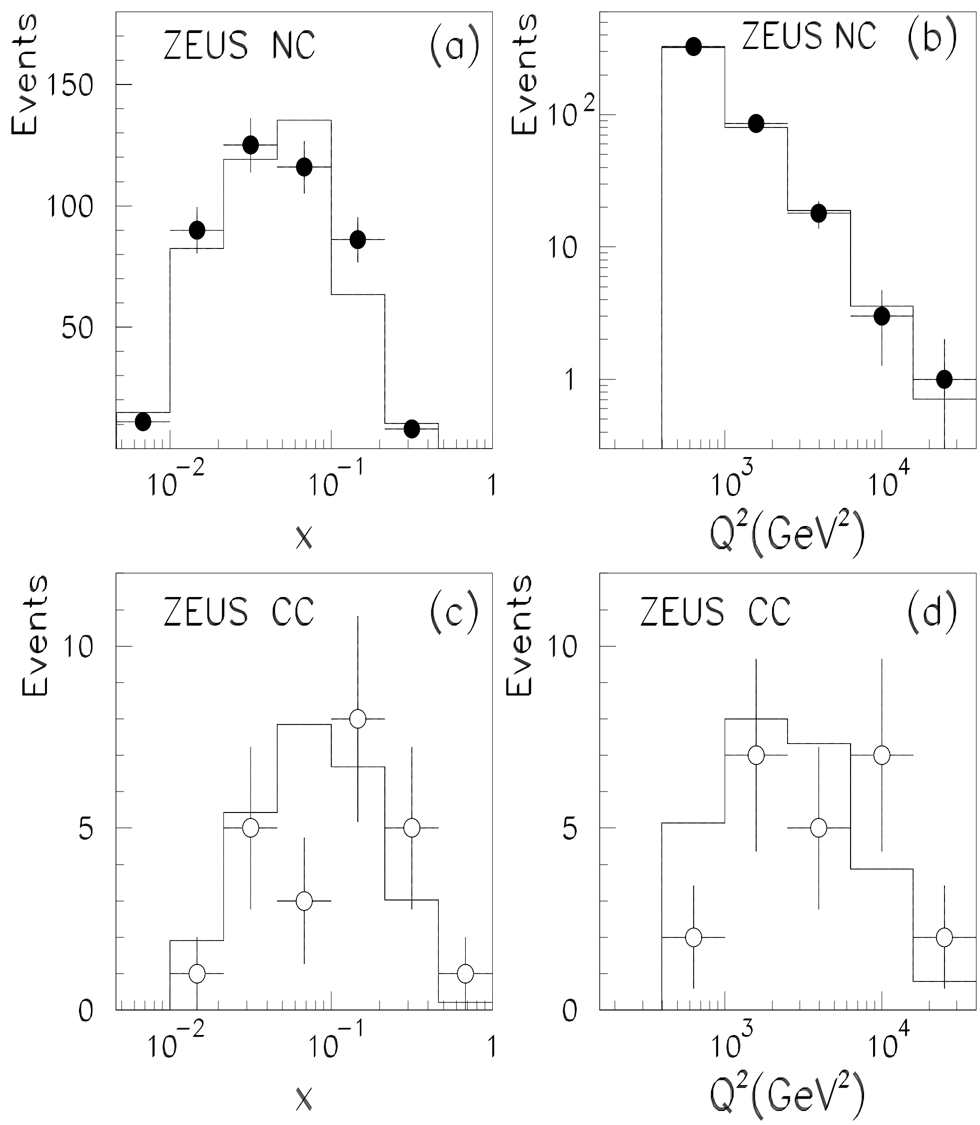

FIG. 1. (a) x for NC events (b) Q^2 for NC events (c) x for CC events (d) Q^2 for CC events. The points with error bars are ZEUS data. The histograms are the predicted numbers of events from the absolutely normalized simulation.

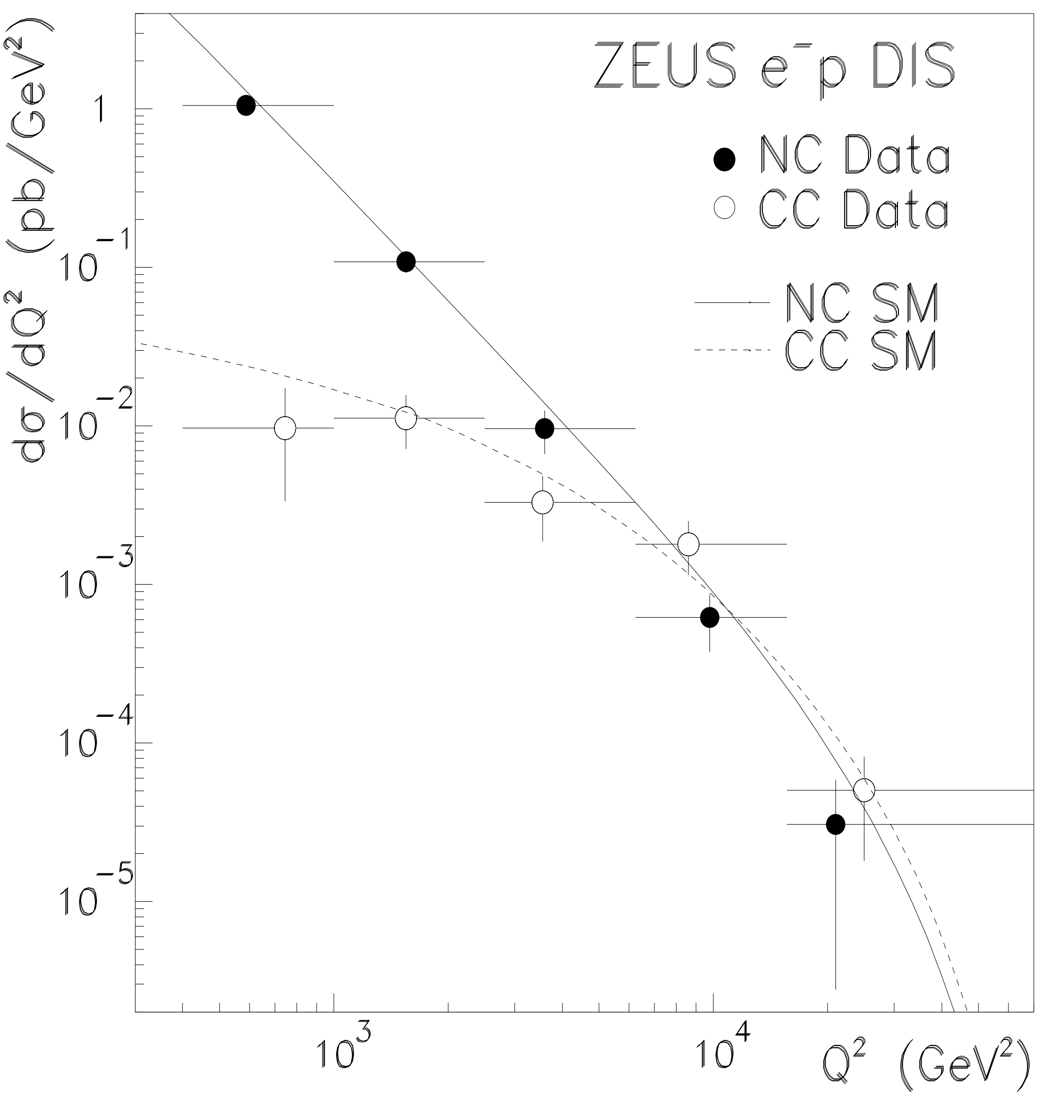

FIG. 2. $d\sigma/dQ^2$ for CC and NC DIS. The points with errors are the data, and the curves are the Standard Model cross sections. The data are plotted at the average Q^2 of the events in each bin.